environmental microbiology

Environmental Microbiology (2018) **20**(5), 1765–1781 doi:10.1111/1462-2920.14106

Fundamental drivers for endolithic microbial community assemblies in the hyperarid Atacama Desert

Victoria Meslier,[1] M. Cristina Casero,[2] Micah Dailey,[1] Jacek Wierzchos,[2] Carmen Ascaso,[2] Octavio Artieda,[3] P. R. McCullough[4] and Jocelyne DiRuggiero[1]*

[1]*Department of Biology, The Johns Hopkins University, Baltimore, MD, USA.*

[2]*Museo Nacional de Ciencias Naturales, CSIC, Madrid, Spain.*

[3]*Departamento Biologica Vegetal, Ecologia y ciencias de la Tierra, Universidad de Extremadura, Plasencia, Spain.*

[4]*Department of Physics and Astronomy, The Johns Hopkins University, Baltimore, MD, USA.*

Summary

In hyperarid deserts, endolithic microbial communities colonize the rocks' interior as a survival strategy. Yet, the composition of these communities and the drivers promoting their assembly are still poorly understood. We analysed the diversity and community composition of endoliths from four different lithic substrates – calcite, gypsum, ignimbrite and granite – collected in the hyperarid zone of the Atacama Desert, Chile. By combining microscopy, mineralogy, spectroscopy and high throughput sequencing, we found these communities to be highly specific to their lithic substrate, although they were all dominated by the same four main phyla, *Cyanobacteria*, *Actinobacteria*, *Chloroflexi* and *Proteobacteria*. Our finding indicates a fine scale diversification of the microbial reservoir driven by substrate properties. The data suggest that the overall rock chemistry and the light transmission properties of the substrates are not essential drivers of community structure and composition. Instead, we propose that the architecture of the rock, i.e., the space available for colonization and its physical structure, linked to water retention capabilities, is ultimately the driver of community diversity and composition at the dry limit of life.

Received 6 September, 2017; accepted 15 March, 2018. *For correspondence. E-mail: jdiruggiero@jhu.edu; Tel. 410-516-8498, Fax 410-516-5213.

Introduction

Often considered as the last refuge for life in extreme deserts, the endolithic – within rock – habitat is ubiquitous in hot, cold and polar deserts around the world (Walker and Pace, 2007; Omelon, 2008; Wierzchos *et al.*, 2012a). The microbial communities found in this habitat are relatively simple and, as such, provide good model systems to elucidate adaptive mechanisms to the dry limit of life (Walker and Pace, 2007). Characterization of the structure and composition of these endolithic communities has shown that they all harbour phototrophic primary producers, co-occurring with a wide range of heterotrophic consumers, and seeded from a 'metacommunity', i.e., a microbial reservoir available for colonization (Walker and Pace, 2007; Wierzchos *et al.*, 2012a). Given the extreme environmental context, several studies have shown that water is the most important factor for survival of endolithic communities in hyperarid deserts. Water can originate from sparse precipitations but also from dew, fog, deliquescence, capillary condensation or snow melt in polar deserts, and its availability is dependent on substrate properties (Friedmann *et al.*, 1988; Omelon *et al.*, 2006; Büdel *et al.*, 2008; Davila *et al.*, 2008; Wierzchos *et al.*, 2012b; Robinson *et al.*, 2015). However, the relationship between substrate properties and the diversity of the communities inhabiting those substrates remains poorly understood.

The capacity of the rock substrate to harbour life, i.e., its bioreceptivity, is determined by its chemical and physical properties (Wierzchos *et al.*, 2012a). The rock environment provides protection against harmful solar irradiance, enhances the water budget by up-taking and retaining water, buffers high thermal fluctuations and provides physical stability to microbial communities (Friedmann, 1980; Friedmann 1982; Walker and Pace, 2007; Wierzchos *et al.*, 2012a). Depending on the structure of the lithic substrate, the colonization zone can be found inside pores beneath the rock surface (cryptoendolithic), in cracks and

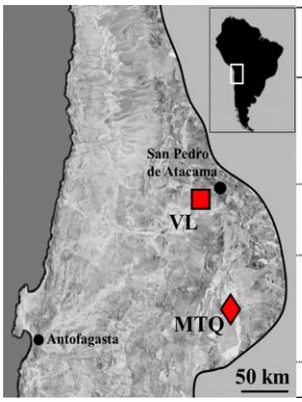

Sampling sites		Valle de la Luna (VL)[a]	Monturaqui (MTQ)[b]
Air Temperature (°C)	Min	-4.4	-4.7
	Ave	**17.3**	**15.0**
	Max	40.9	49.3
PAR (µmol s^{-1} m^{-2})	Ave	**810.9**	**1178.5**
	Max	2423.7	2553.7
Air RH (%)	Min	4.6	1.0
	Ave	**21.2**	**18.3**
	Max	96.4	100.0
Rainfall [c]	mm/y	**27.8**	**24.5**

Fig. 1. Sampling locations in the Atacama Desert and microclimate data. Map of the Atacama Desert in Chile, with sampling locations: VL, Valle de la Luna (red square) and MTQ, Monturaqui area (red diamond). [a]Data recorded from April 2013 to December 2015 (32 months – this article); [b]data from January 2011 to February 2013 (22 months) (Wierzchos *et al.*, 2015); [c]data extracted from DiRuggiero and colleagues (2013) and (Wierzchos *et al.*, 2015). [Colour figure can be viewed at wileyonlinelibrary.com]

fissures (chasmoendolithic) or inside pores in the bottom part of the rock (hypoendolithic) (Golubic *et al.*, 1981; Wierzchos *et al.*, 2011).

In hyperarid deserts, endolithic microbial communities have been found to colonize a number of rock substrates, including carbonates (de los Ríos *et al.*, 2004; Horath *et al.*, 2006; Tang *et al.*, 2012; 2016; DiRuggiero *et al.*, 2013; Crits-Christoph *et al.*, 2016a; Kidron and Temina 2017), gypsum (Dong *et al.*, 2007; Ziolkowski *et al.*, 2013; Wierzchos *et al.*, 2015), gypsum crust (Hughes and Lawley, 2003; Stivaletta *et al.*, 2010; Wierzchos *et al.*, 2011; Canfora *et al.*, 2016), halite (Wierzchos *et al.*, 2006; Davila *et al.*, 2008; de los Ríos *et al.*, 2010; Robinson *et al.*, 2015), ignimbrite (Wierzchos *et al.*, 2013; Cámara *et al.*, 2014), granite (Friedmann and Kibler 1980; Friedmann 1982; de los Ríos *et al.*, 2005; 2007; Büdel *et al.*, 2008; Li *et al.*, 2013) and sandstone (Friedmann 1982; McKay and Friedmann, 1985; Wierzchos and Ascaso, 2001; Ascaso and Wierzchos, 2002; de los Ríos *et al.*, 2004; Pointing *et al.*, 2009; Archer *et al.*, 2017). The great variety of rocks supporting endolithic life shows the versatility of microorganisms to colonize a wide array of substrates and their incredible potential for adaptation to extreme environmental conditions.

Although culture-independent methods combined with microscopy techniques have led to a more complete understanding of endolithic communities and their habitat, a broader picture of the endolithic community structures and compositions is still lacking. Indeed, most of the studies have focused on one or two rock substrates at a time, making direct comparisons across substrates difficult, if not impossible at the molecular level. In this study, we conducted a large-scale analysis of the composition of 47 endolithic microbial communities found in calcite, gypsum, ignimbrite and granite rocks collected in the same climate regime of the Atacama Desert. We combined field measurements, microscopy, geochemical characterization, spectroscopic measurements and 16S rDNA amplicon high-throughput sequencing to address the communities' specific features and identify the drivers promoting their assembly. Within the same climate regime, we found endolithic communities highly specific to their substrates, suggesting a fine scale diversification of the available microbial reservoir.

Results

We combined microclimate measurements, mineralogy, spectroscopic and microscopy analyses and high throughput culture-independent molecular data to identify the factors underlying the structure and composition of microbial assemblages in endoliths from the hyper arid Atacama Desert. Illumina sequencing of 47 samples resulted in a total of 1,773,072 V3-V4 SSU rDNA reads, with an average number of paired-end reads per sample of 17 469 ± 4375 and an average length of 452 ± 11 bp, providing an unprecedented level of detail for these communities. Slopes of the rarefaction curves indicated that most of the community was sampled at the 3000-sequence read level (Supporting Information S5).

Microclimate data

Forty-seven samples from 4 different rock substrates were collected from two sampling sites, Valle de la Luna area (VL) and Monturaqui area (MTQ), located in the hyperarid zone of the Atacama Desert (Fig. 1 and Supporting Information S1). Climate data were recorded over a period of 22 months or more, showing similar climate regimes for both sites (Fig. 1). The mean air temperature was about 16°C, with strong amplitude between minima and maxima (from −4°C to 49°C). The average diurnal PAR (Photosynthetically Active Radiation) was ∼ 1000 µmol photons m^{-2} s^{-1} with a maximum of 2553.7 µmol photons m^{-2} s^{-1}, substantiating the extremely intense solar irradiance found in this region (Cordero *et al.*, 2014). Both sites experienced extremely dry conditions, with an average air relative humidity (RH) of about 20% with frequently lows of ∼ 5% and 1% in VL and MTQ respectively. Precipitations were extremely scarce with mean annual values of 24.5 and

Table 1. Mineralogical composition of rock substrates obtained by XRD.

Substrate	XRD analysis	Chemical formula	References
Calcite	Calcite (100%)	$CaCO_3$ (100%),	DiRuggiero *et al.*, 2013
Gypsum	Gypsum (96%–98%), cristobalite, calcite, potassium feldspar (2%–4%)	$CaSO_4{\cdot}2H_2O$ (96%–98%), SiO_2, $CaCO_3$, $KAlSi_3O_8$	Wierzchos *et al.*, 2015
Ignimbrite	Andesine (51%), disordered sodian anorthite (42%), biotite (7%)	(Ca, Na)(Al, Si)$_4O_8$ (51%), $CaAl_2Si_2O_8$ (42%), $K(Mg,Fe)_3AlSi_3O_{10}(OH)_2$ (7%)	Wierzchos *et al.*, 2013
Granite	Quartz (25%) potassium feldspar (22%) plagioclase (34%), biotite (16%) other (3%)	SiO_2 (25%), $KAlSi_3O_8$ (22%),$K(Mg,Fe)_3AlSi_3O_{10}(OH)_2$ (6%), other (3%)	this study

27.8 mm/y in MTQ and VL respectively. Although this level of precipitation might seem high for the Atacama Desert, the Aridity Index (AI = rainfall precipitation/mean annual potential evapotranspiration) was previously calculated to ~ 0.0095 and ~ 0.0075 for VL and MTQ respectively (DiRuggiero *et al.*, 2013, Wierzchos *et al.*, 2013), placing these sampling sites far below the threshold of 0.05 used to define the world's hyperarid zones (Houston and Hartley, 2003).

Mineralogy of the substrates

X-ray diffraction (XRD) analysis showed that the samples collected in VL were sedimentary carbonate rocks composed of calcite (Table 1). In the MTQ area, the gypsum rocks were mainly composed of calcium sulfate with minor minerals such as cristobalite, calcite and potassium feldspar. These evaporitic rocks also contained the mineral sepiolite. In contrast, the mineral composition of the ignimbrite and granite rocks was more complex with the pyroclastic ignimbrite rocks composed of andesine, disorded sodian anorthite and biotite. The granite rocks were composed of quartz, potassium feldspar with small amounts of plagioclase and biotite. The water-soluble ions measured for each of the substrate type were remarkably low, regardless of the chemical complexity of the substrate, and often close to the detection limits of the ICP and IC methods (Supporting Information S3A).

Total water retention capacity and porosity

Total water retention capacity (TWRC) and porosity were measured by total immersion of rocks into water. While chasmoendolithic substrates (granite and calcite) had low TWRC [0.3% and 1.65% (w/w) respectively] and low porosity values [0.8% and 2.75% (v/v) respectively], higher estimates were found for cryptoendolithic substrates [TWRC of 11.3% and 10.7% (w/w) and porosity values of 17% and 12.15% (v/v) for ignimbrite and gypsum respectively]. Analysis performed on multiple samples of gypsum and calcite showed the high heterogeneity of TWRC and porosity measurements between rocks of the same substrate, especially for calcite samples (Supporting Information S3B).

Substrate light transmission properties

Light transmission spectra were obtained for each of the four substrates by measuring the relative solar irradiance from approximately 350–950 nm at 2 mm below the rocks' surfaces (Fig. 2 and Supporting Information S4). We used solar light and a Fresnel lens to concentrate enough light to obtain high signal to noise spectra. A cosine corrector was used for these measurements, providing a 180° field of view to the light sensor. This was essential to capture both the light entering the rock perpendicular to the sensor and the light scattering throughout the substrate, resulting from the minerals' light properties, fissures, cracks and pores in the rock. Our data showed that spectral transmission varied greatly across substrates with values from 7% to less than 0.001% of incident solar light at 665 nm (max

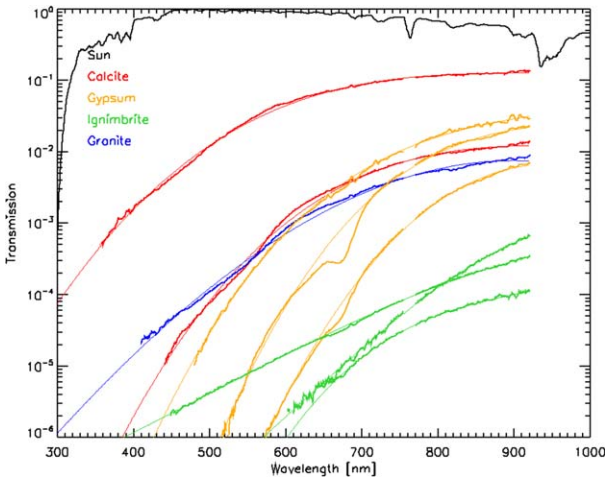

Fig. 2. Light transmission spectra at the nominal depth of 2 mm from the surface of the rocks for calcite, granite, gypsum and ignimbrite. Thick coloured lines are data and thin coloured lines are polynomial fits to the data. Microorganisms in the rocks were exposed to an irradiance proportional to the product of the solar spectrum (black line) and their individual transmission curve (coloured lines). Black, solar spectrum with its peak normalized to 1 on the *y* axis; red, calcite; blue, granite; orange, gypsum; green, ignimbrite. The telluric molecular oxygen band at 760 nm was masked. [Colour figure can be viewed at wileyonlinelibrary.com]

Table 2. Characteristics of endolithic colonization zones.

Sampling site		Valle de la Luna		Monturaqui	
Substrate		Calcite	Gypsum	Ignimbrite	Granite
Type of colonization		CH	CR and CH	CR	CH
Number of samples		16	19	7	5
Width and depth of colonization zone	Min depth from surface (mm)	2 ± 1.3	1.3 ± 0.75	0.8 ± 0.3	1.25 ± 0.6
	Ave width (mm)	7 ± 4.8	2.4 ± 1.15	1.1 ± 0.5	3.8 ± 1.8
	Max depth from surface (mm)	9.6 ± 7.6	3.2 ± 1.5	1.9 ± 0.7	5.1 ± 1.5

Reported for each substrate are the type of colonization (CR, cryptoendolithic; CH, chasmoendolithic), the number of samples, and the width, minimum and maximum depth of colonization in mm (minimum and maximum depths were measured from top surface). Values are the results of 3 measurements per individual rock for at least 4 rocks per substrate.

absorption wavelength for chlorophyll a), at 2 mm below the rock surface (Fig. 2). Measurements from multiple rocks revealed the heterogeneity of each substrate with, for example, transmission values ranging from 7% to 0.3% of incident sun light at 665 nm for calcite. Nevertheless, a trend was observed with calcite being the most translucent substrate, followed by granite, gypsum and with ignimbrite being the least translucent (Fig. 2). While our measurements were made 2 mm below the rock surface for comparison purposes, it is, however, important to relate light transmission properties with depth of colonization for each substrate. While we did not measure experimentally light transmission at the colonization zone, because of the difficulty in drilling rocks to less than 2 mm from their surfaces without the rocks crumbling apart, we found that our spectral data inversely correlates with the colonization zone depths reported in Table 2, supporting the idea that light could be seen as a 'positional driver' of the endolithic community.

We also observed that all wavelengths were not transmitted equally through the rock substrates, with significantly higher transmission in the red than in the blue wavelengths (400–500 nm). Not surprisingly, we also found that all substrates blocked near UV light at 2 mm depth (the calibrated transmission was $< 10^{-3}$ at wavelengths less than 350 nm for all substrates). Additionally, spectral measurements at increasing depths from the surface within the same rock for the gypsum and ignimbrite substrates showed a decreased in light transmission, validating our expectations that less light was transmitted to 4 mm depth than 2 mm depth (Supporting Information S4).

Endolithic colonization zones

Cross sections of the rocks revealed a significant heterogeneity in the micromorphology and structure of the lithic substrates (Fig. 3A1–D1, Table 2). Calcite rocks, composed of laminated layers covered by a hard surface layer with microrills (DiRuggiero *et al.*, 2013), displayed large irregular fissures and cracks perpendicular or parallel to the rock surface, with a green colonization zone as deep as 1.5 cm (Fig. 3A1, Table 2). Microbial cells were organized in large clusters along the cracks and fissures of this substrate and adhered to different minerals without preference (Fig. 3A2). SEM-BSE revealed dense arrangements of cyanobacterial cells embedded in concentric sheets of extracellular polymeric substance (EPS) that were filled by heterotrophic bacteria (Fig. 3A3). The colonization zone within gypsum was mostly cryptoendolithic, close to the compact gypsum surface layer, and two characteristic pigment layers, orange for carotenoids and green for chlorophylls, were organized with depth (Wierzchos *et al.*, 2015; Vítek *et al.*, 2016) (Fig. 3B1, Table 2). *Cyanobacteria* were found among lenticular gypsum crystals, filling up vertically elongated pores, and aggregated around sepiolite nodules (Fig. 3B2). This clay mineral, with high water retention capacity, was previously identified in gypsum by Wierzchos and colleagues (2015). Detailed SEM-BSE image of the gypsum (Fig. 3B3) showed *Cyanobacteria* with different micromorphology (larger cells) accompanied by heterotrophic bacteria. Ignimbrite rocks had a consistent and narrow cryptoendolithic colonization zone, characterized by a vitrified foam-like structure under a brown-coloured varnish covering the rock surface (Fig. 3C1, Table 2) (Wierzchos *et al.*, 2013). Microscopically, this substrate showed small elongated vesicles among a glass shards matrix. Cells filled these narrow spaces, while others, not connected to the surface, showed no signs of microbial colonization (Fig. 3C2). Detailed SEM-BSE view revealed dense cyanobacterial aggregates and heterotrophic bacteria attached to the glass shards (Fig. 3C3). Granite rocks, devoid of a surface crust, had a dark green chasmoendolithic colonization within random arranged fissures and cracks under the rock surface (Fig. 3D1). Dense microbial aggregates were found among grains of quartz and feldspars (Fig. 3D2). A detailed view showed cyanobacterial cells associated with rod shape heterotrophic bacteria (Fig. 3D3).

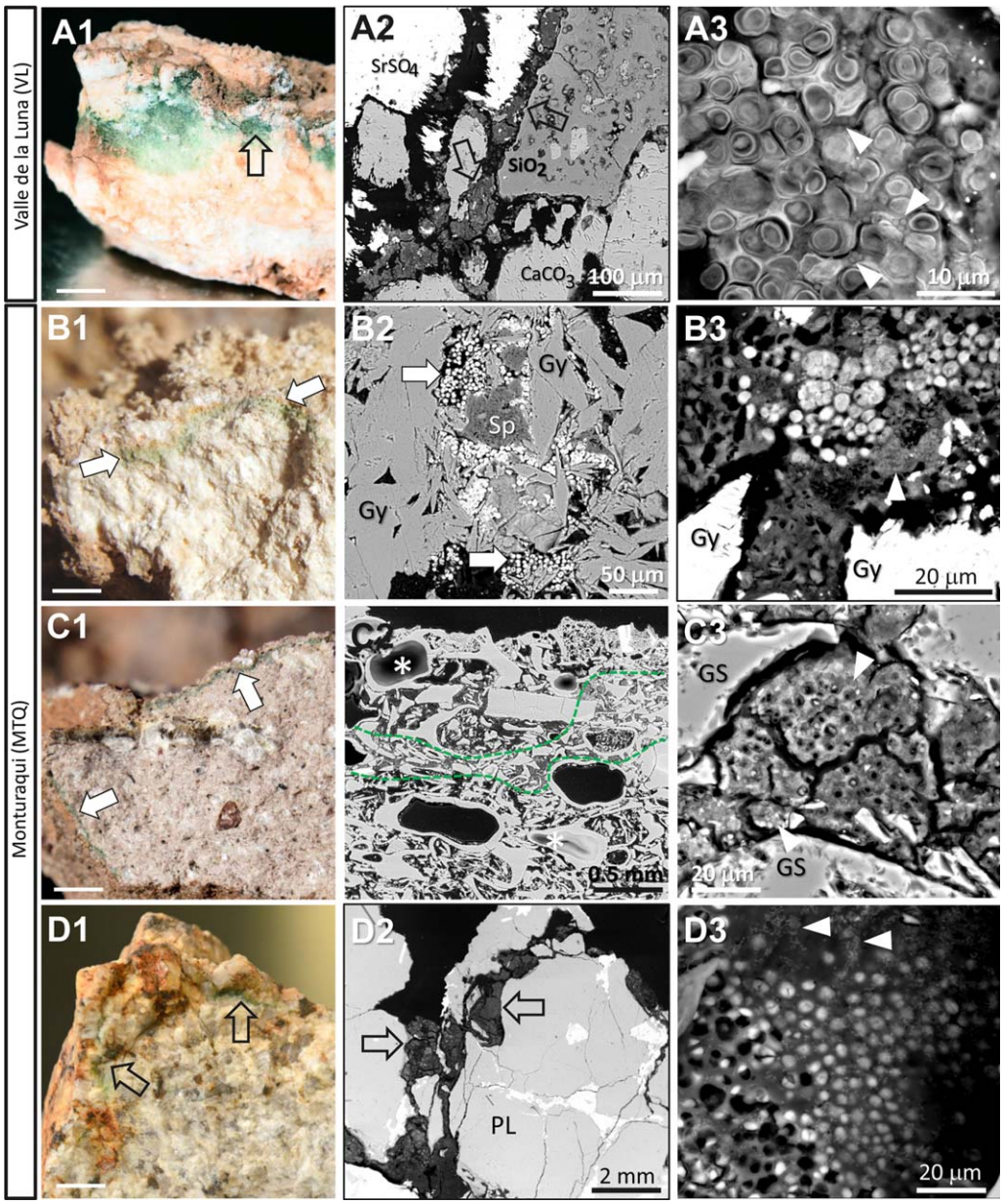

Fig. 3. Cross-sections and SEM-BSE images of endolithic colonization zones for calcite (A), gypsum (B), ignimbrite (C) and granite (D). (A1–D1) cross-sections of colonized rocks with variation in depth, width, distribution and colour of the endolithic habitats; open black and filled white arrows indicates chasmoendolithic (A1 and D1) and cryptoendolithic (B1 and C1) habitats respectively; scale bars: 1 cm. Series A2–D2 and A3–D3 shows SEM-BSE images revealing aggregates of endolithic communities inside the cracks and pores of the lithic substrates; (A2 and A3) fissures within calcite filled by chasmoendoliths between celestine ($SrSO_4$), silica (SiO_2) and calcite ($CaCO_3$) minerals; (B2 and B3) aggregates of cyanobacteria among gypsum (Gy) crystals and surrounding sepiolite (S) nodules; (C2 and C3) aggregates of cyanobacteria within bottle shape pores of ignimbrite, green lines represent the cryptoendolithic colonization zone; and (D2 and D3) dense cyanobacterial cell aggregates within cracks of granite. White arrowheads indicated heterotrophic bacteria associated to cyanobacterial aggregates. [Colour figure can be viewed at wileyonlinelibrary.com]

Structure and composition of endolithic communities

High throughput sequencing of 16S rDNA amplicons was used to characterize communities across 47 samples and 4 substrates. Diversity metrics, calculated from OTUs clustered at 97%, revealed two significantly different groups of substrates with high and low diversity (T statistic = 10.8, p value < 0.0001) (Supporting Information S5). The granite and ignimbrite substrates grouped at the lower end of diversity (< 220 OTUs; Shannon index < 5) with no significant differences in alpha diversity indices (Observed Richness; T-statistic = 1.52, p value = 0.17). In contrast, the calcite and gypsum substrates harboured high diversity

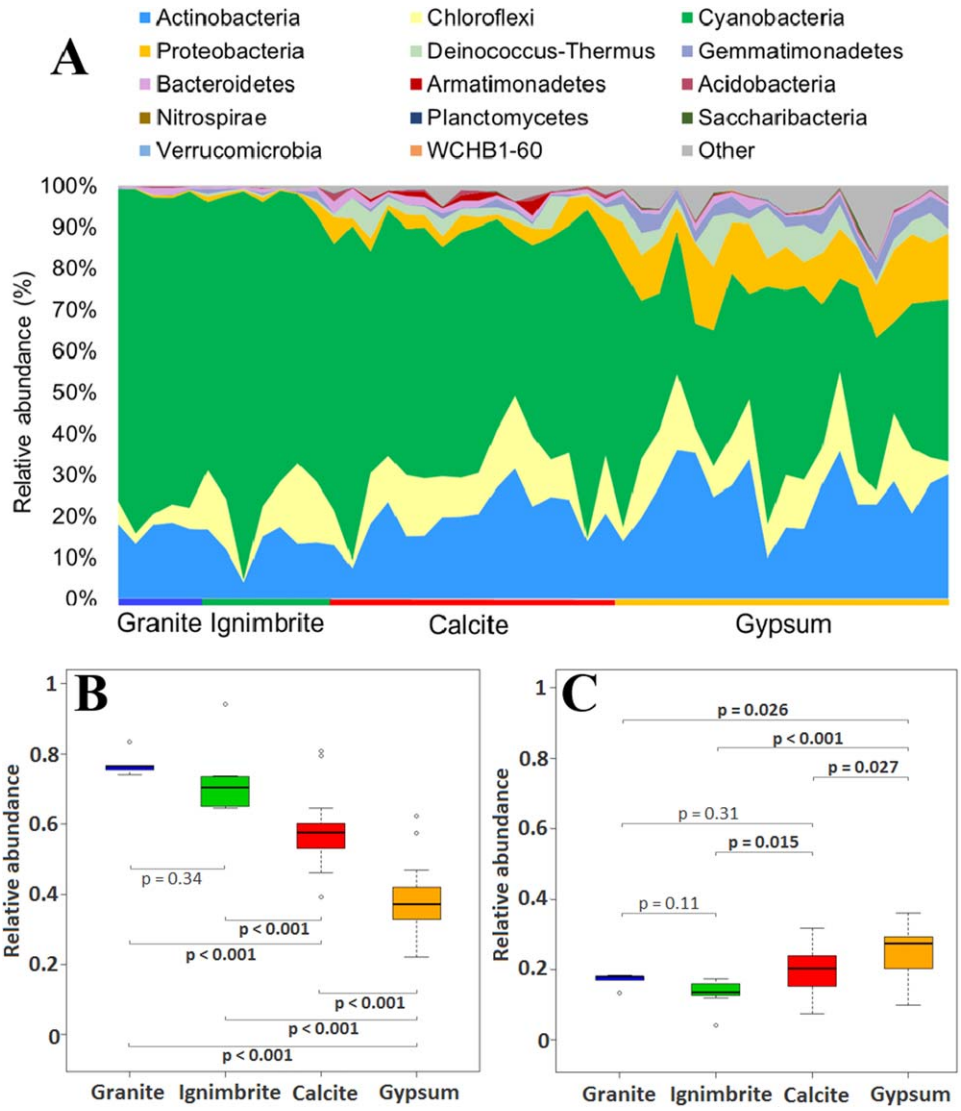

Fig. 4. Composition of endolithic microbial communities. A total of 14 phyla were found using the V3-V4 region of the 16S rRNA gene with OTUs clustering at 97%. A. Relative abundance (%) of phyla detected across all samples, others indicate unassigned reads. Boxplots of relative abundance for *Cyanobacteria* (B) and *Actinobacteria* (C) per substrate-type; one-way ANOVA p values were 2×10^{-11} and 4×10^{-4} for *Cyanobacteria* and *Actinobacteria* respectively; p values from a t test analysis are reported for each pairs of substrate (bold; p value < 0.05); granite is in blue, ignimbrite in green, calcite in red and gypsum in orange. [Colour figure can be viewed at wileyonlinelibrary.com]

(> 400 OTUs; Shannon index ~ 6) and significant differences in their observed richness (Tstatistic = 2.57, p value = 0.016). It is notable that the gypsum and ignimbrite substrates, collected side by side in the field (photo in Supporting Information S1), had the highest (545) and lowest (126) number of OTUs respectively.

A total of 14 bacterial phyla were found across all substrates and distinct high-ranked taxon dominated. *Cyanobacteria*, *Actinobacteria*, *Chloroflexi* and *Proteobacteria* were the most abundant phyla, representing 86%–98% of the total community (Fig. 4A). *Cyanobacteria* dominated the communities in all substrates (Fig. 4B) with relative abundance of ~ 40% in gypsum, ~ 60% in calcite and of more than 70% in granite and ignimbrite. *Actinobacteria* was the second most abundant phylum but never exceeded 30% of the total community composition (Fig. 4C). One-way ANOVA confirmed significant differences of the mean relative abundance for the 4 main phyla across substrates (Fig. 4 and Supporting Information S6). Analysis of means further revealed that the relative abundance of *Chloroflexi* was significantly different in the granite and ignimbrite communities but that *Cyanobacteria*, *Actinobacteria* and *Proteobacteria* was not. Additionally, the relative abundance of *Actinobacteria* was similar in granite and calcite, while no significant difference was found in the relative abundance of *Chloroflexi* in ignimbrite, calcite and gypsum communities. *Deinococcus*, *Gemmatimonadetes, Bacteroidetes* and *Armatimonadetes* were found in all substrates at relatively low abundance, between 1% and 5%, with higher levels in calcite and gypsum. Six phyla, *Acidobacteria*, *Saccharibacteria*, *Nitrospirae*, *Planctomyces*, *Verrucomicrobia* and candidatus WHCB1–60, were found at very low abundance, ≤ 1%, in calcite and gypsum and sporadically detected in granite and ignimbrite (Supporting Information S7). Strong anti-correlations of the relative abundance of *Cyanobacteria* were found with that of *Actinobacteria* and *Proteobacteria* ($rho_{spearman} = -0.821$ and

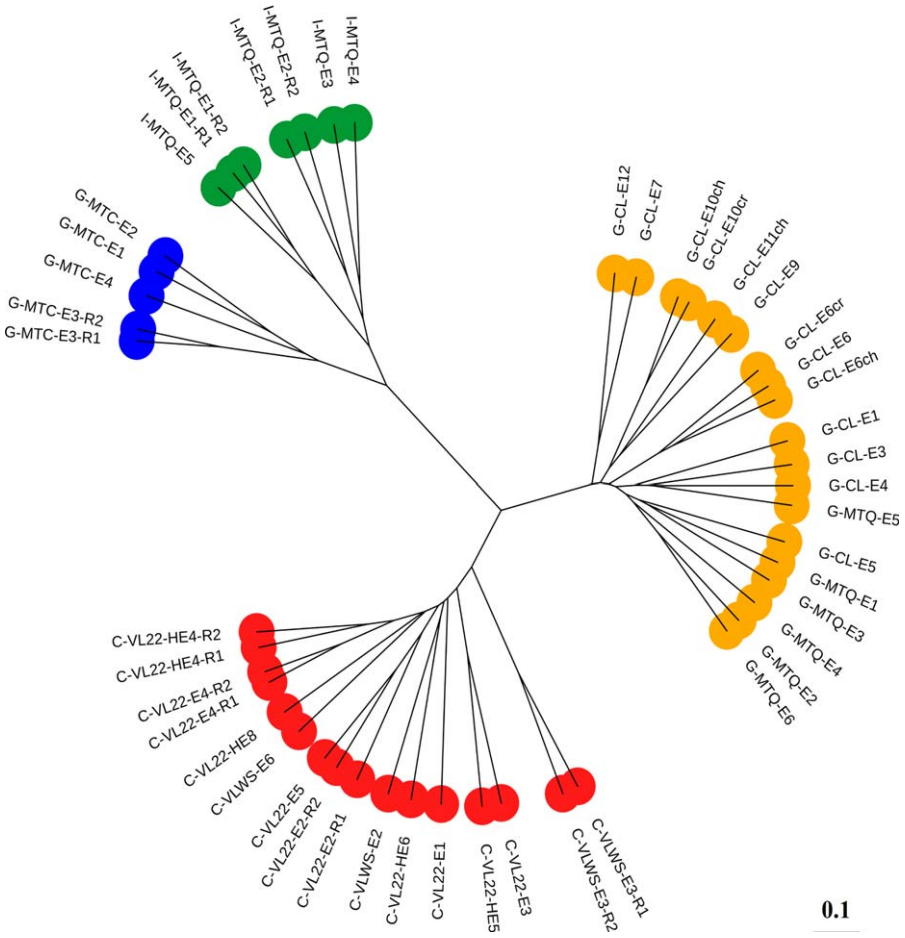

Fig. 5. Clustering of endolithic communities by substrate-type. Unweighted Pair Group Method with Arithmetic Mean (UPGMA) dendrogram was constructed using Bray-Curtis dissimilarity indices and visualized using iTOL. Granite in blue, ignimbrite in green, calcite in red and gypsum in orange. Scale bar indicates 10% dissimilarity between samples. [Colour figure can be viewed at wileyonlinelibrary.com]

-0.850 respectively, p values $< 1 \times 10^{-4}$) and *Chloroflexi* ($rho_{spearman} = -0.459$, p value $= 0.001$) for all substrates (Fig. 4 and Supporting Information S6). Diversity metrics were also strongly anti-correlated with the abundance of *Cyanobacteria* ($rho_{spearman} = -0.718$ and -0.833 for observed richness and Shannon indexes respectively, p values $< 1 \times 10^{-4}$), while these metrics were positively correlated to the abundance of the other 3 main phyla ($rho_{spearman}$ = from 0.308 to 0.758, p values from 1×10^{-4} to 0.03).

Only one archaeal OTU was detected in our data at very low abundance (0.007%) and was filtered out from our quality-controlled dataset because of potential sequencing errors. This absence of archaeal lineages is interesting – but not surprising – as previous work on lithic microbial communities have also reported the absence or extremely low abundance, of archaea in these habitats (Pointing *et al.*, 2009; DiRuggiero *et al.*, 2013), with the exception of endolithic halite communities (Crits-Christoph *et al.*, 2016b; Finstad *et al.*, 2017).

Partitioning of diversity

We further examined the endoliths' community composition at a higher level of resolution using Beta-diversity analyses. A hierarchical clustering analysis revealed that, based on community composition, the samples clustered into 4 distinct groups according to substrate type (Fig. 5). The ignimbrite and granite samples were the least distant from each other, which was consistent with their low observed richness, whereas gypsum samples were as distant to the ignimbrite/granite samples as the calcite samples were, regardless of their proximity in the field (Fig. 5). This substrate-type grouping was supported by PCoA plots generated from unweighted and weighted UniFrac distance matrices (Supporting Information S8). Adonis and ANOSIM tests, performed with substrate categories, confirmed the statistical significance of the grouping ($R^2 = 0.61$ and $R = 0.99$ with p values $= 0.001$ for adonis and ANOSIM respectively).

Despite *Cyanobacteria* being the most abundant phyla across all substrates, it was less diverse phylogenetically than *Actinobacteria* (161 vs. 426 OTUs). A fine-scale analysis of the most abundant *Cyanobacteria* ($n = 50$ OTUs) and *Actinobacteria* OTUs ($n = 129$ OTUs), comparing their relative abundance across samples, revealed clusters of OTUs preferentially associated with substrate types (Fig. 6A and Supporting Information S9). To test the statistical

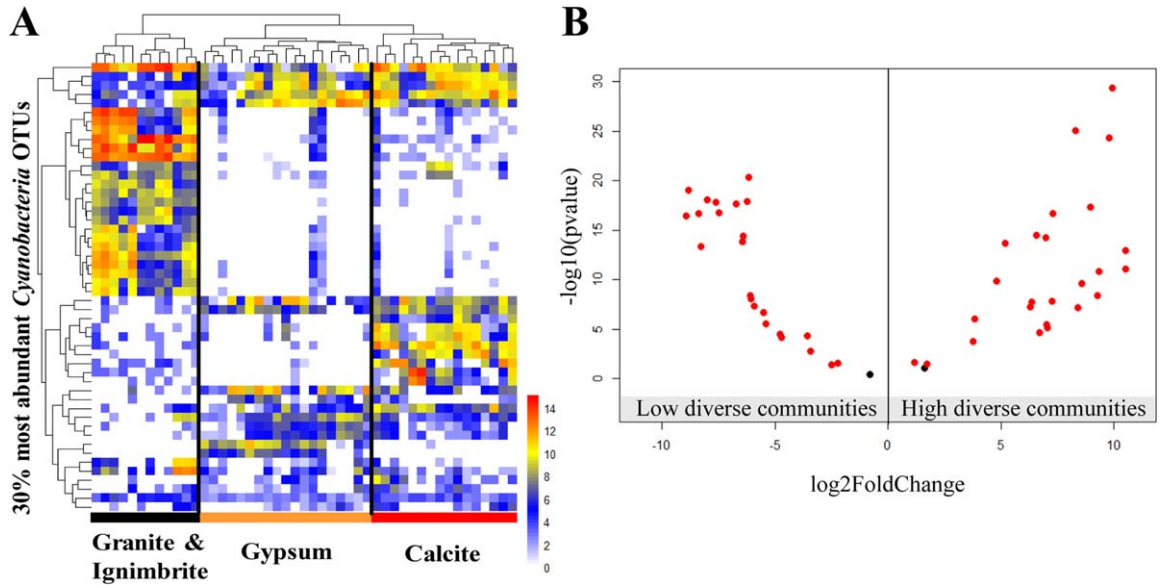

Fig. 6. Differential abundance of the 30% most abundant *Cyanobacteria* OTUs ($n = 50$).
A. Heatmap of *Cyanobacteria* OTUs clustered by sample (columns) and relative abundance (rows). Colour scales refer to the normalized abundance of each OTU across samples (log-transformed for visualization purposes). Granite and ignimbrite samples are in black, calcite in red and gypsum in orange.
B. Volcano plots of *Cyanobacteria* OTUs in low (granite and ignimbrite) and high (gypsum and calcite) diversity endolithic communities. The $\log_2$ fold change, calculated for each OTU using DESEq2, was plotted against the adjusted negative log10 *p* values (red; FDR *p* value < 0.05, black; FDR *p* value > 0.05). [Colour figure can be viewed at wileyonlinelibrary.com]

basis of this observation, we performed a differential abundance analysis using DESeq2 between the high (gypsum and calcite; >400 OTUs) and low (ignimbrite and granite; <220 OTUs) diversity groupings defined above by alpha diversity metrics (Supporting Information S5). All *Cyanobacteria* OTUs, except for 2, were significantly assigned to either the low ($n = 23$) or the high diversity groups ($n = 25$) (FDR *p* values < 0.05; Fig. 6B), supporting the clusters visualized in Fig. 6A. Similarly, top *Actinobacteria* OTUs were significantly assigned to either the low ($n = 14$) or the high ($n = 86$) diversity groupings, whereas 29 of them could not be significantly assigned (Supporting Information S9).

A phylogenetic analysis of the major *Cyanobacteria* OTUs showed that most were assigned to *Chroococcidiopsis* ($\sim$ 70% of the OTUs) (Supporting Information S10). *Actinobacteria* OTUs were mainly identified as members of the *Solirubrobacter, Rubrobacter, Actinobacterium, Euzebya, Microlunatus, Molestobacter* and *Geodermatophilus* genera (Supporting Information S10). Both maximum likelihood trees showed that substrate-specific clusters of OTUs, in the low and high diversity communities, had members belonging to similar taxonomic groups.

Discussion

In this study, we addressed the drivers promoting the assembly of endolithic microbial communities in four different substrates from the same hyperarid climate regime of the Atacama Desert. The rocks were collected within a small geographic area and sometimes even side by side in the field. While previous studies have demonstrated the impact of climate regime, in particular the availability of atmospheric water, in shaping the structure of lithic communities (Friedmann *et al.*, 1988; Cockell *et al.*, 2002; Pointing *et al.*, 2007; Büdel *et al.*, 2008; Davila *et al.*, 2008; Stomeo *et al.*, 2013; Robinson *et al.*, 2015), most studies have only focused on one or two types of rock substrates and often reported limited data on community diversity and composition. For example, the diversity of microbial communities in calcite rocks (DiRuggiero *et al.*, 2013) and halite nodules (Robinson *et al.*, 2015) from the Atacama Desert was found to be strongly correlated with atmospheric moisture. Similarly, shifts in community diversity and structure were reported for quartz hypoliths along moisture transects in China and Namib deserts (Pointing *et al.*, 2007; Stomeo *et al.*, 2013). To our knowledge, no study has compared community assembly over a wide range of endolithic substrates – sedimentary, evaporitic, volcanic and igneous – and without the confounding effect of different climate regimes in a hyperarid desert. We also provided for the first time the composition and structure of granite endolithic microbial communities from the Atacama Desert, although hypolithic granite colonization was previously reported but never investigated at the molecular and/or microscopic levels (Warren-Rhodes

et al., 2006), in contrast from samples from Antarctica and China (Friedmann and Kibler, 1980; Friedmann, 1982; de los Ríos *et al.*, 2005; 2007; Büdel *et al.*, 2008; Li *et al.*, 2013; Archer *et al.*, 2017).

Our analysis, using an unprecedented sequencing depth for these types of communities, revealed a similar microbial community structure across substrates at the phylum level, which is consistent with previous studies of endolithic communities from multiple deserts (de la Torre *et al.*, 2003; Walker *et al.*, 2005; Dong *et al.*, 2007; Pointing *et al.*, 2007; Azúa-Bustos *et al.*, 2011; DiRuggiero *et al.*, 2013; Li *et al.*, 2013; Crits-Christoph *et al.*, 2016a,b; Armstrong *et al.*, 2016; Lee *et al.*, 2016; Archer *et al.*, 2017; Lacap-Bugler *et al.*, 2017) and suggests that these phyla constitute an ubiquitous 'metacommunity' available for the colonization of lithobiontic substrates (Walker and Pace, 2007; Wierzchos *et al.*, 2018). Indeed, the most abundant taxa at the OTU level all belonged to genera recognized for their resistance to desiccation, radiation and oligotrophic conditions found in hyperarid deserts (Friedmann and Ocampo-Friedmann, 1995; Potts, 1999; Billi *et al.*, 2000; Bull, 2011; Krisko and Radman, 2013; Mohammadipanah and Wink, 2016; Lebre *et al.*, 2017). Our data recapitulate previous findings on the pivotal role for *Cyanobacteria* as primary producers in endolithic communities (Friedmann, 1980; 1982; Bell, 1986; Walker and Pace, 2007; Wierzchos *et al.*, 2012a; de los Ríos *et al.*, 2014; Lacap-Bugler *et al.*, 2017) and the idea that variations in *Cyanobacteria* relative abundance between substrates might reflect differences in ecosystem functioning (Cary *et al.*, 2010; Valverde *et al.*, 2015). For example, it was proposed that a higher relative abundance of photoautotrophs in the driest environments might indicate reduced capacity for primary production, due to the scarcity of water, hence the decrease in consumers' relative abundance (DiRuggiero *et al.*, 2013; Robinson *et al.*, 2015; Wierzchos *et al.*, 2018). Indeed, salt deliquescence in halite nodules, and, therefore, conditions conducive to photosynthesis, was continuous in the Salar Grande area of the Atacama Desert while the interior of halite nodules in the driest Yungay area remained wet for only 5362 h per year (Wierzchos *et al.*, 2012b; Robinson *et al.*, 2015), matching a higher relative abundance of phototrophs in the Yungay community (Robinson *et al.*, 2015). Similarly, harsher conditions in the ignimbrite endolithic habitat, when compared to that of calcite, was previously suggested as the motivation for increased *Cyanobacteria* relative abundance (Crits-Christoph *et al.*, 2016a). Here, using a large data set with four different endolithic habitats, we recapitulated those anti-correlations between relative abundance of *Cyanobacteria* and community richness and diversity and with major heterotrophic phyla of the community. For example, endolithic communities from granite and ignimbrite rocks displayed low richness and diversity but high *Cyanobacteria* relative abundance, suggesting a more extreme environment in these substrates. In contrast, calcite and gypsum communities displayed a higher richness and diversity but a lower *Cyanobacteria* relative abundance.

While phylum-level taxa dominated in the four types of substrates, patterns of OTUs' relative abundance from *Cyanobacteria* and *Actinobacteria* demonstrated preferential association of OTUs with the type of substrate. This partitioning at the OTU phylogenetic level was not recapitulated at higher taxonomic ranks suggesting differential adaptation of close relatives to the substrate's physical and chemical properties. Substrate-dependent patterns of community structure have been reported for hypolithic quartz and endolithic sandstone communities from the Dry Valleys, Antarctica (Pointing *et al.*, 2009) and for sandstone communities from the Colorado Plateau, USA (Lee *et al.*, 2016). In all cases, while the hypolithic communities were recruited from the surrounding soils, habitat filtering shaped the assembly of the rock communities (Pointing *et al.*, 2009; Makhalanyane *et al.*, 2013; Lee *et al.*, 2016). Community assembly controlled by the substrate was also observed for the hypolithic colonization of meteorites found in Nullarbor Plain, Australia (Tait *et al.*, 2017). While not from deserts, partitioning of *Cyanobacteria* was reported for microbial communities in dolomite and limestone substrates, demonstrating mineral preferences of euendolithic communities at the OTU phylogenetic level (Couradeau *et al.*, 2017). Using a sampling strategy that minimized the effect of biogeography and atmospheric water input, our large-scale analysis of four different lithic substrates provides further strong evidence for fine scale diversification of endolithic communities, selectively recruited from a microbial reservoir. While the differences in community composition between the calcite and gypsum communities, which have similar diversity metrics, might be attributed to biogeography, it is highly unlikely in view of the arguments presented below and because the sampling locations are only separated by 100 km without any major topological features between them.

The capacity of a lithic substrate to harbour life, i.e., its bioreceptivity, is linked to its chemical, mineralogical and physical properties that provide and maintain sufficient stability and favourable conditions inside the substrate (Walker and Pace, 2007; Wierzchos *et al.*, 2012a). Although mineral composition was found to be significantly different between substrates, and suggested a potentially more complex nutrient supply in granite and ignimbrite rocks, low amounts of water soluble ions were detected independent of the substrates' mineralogy. It is important to note here that there is no standard method for this type of measurement and that the methodology itself can influence the outcome (Sawyer *et al.*, 2000; Toner *et al.*, 2013). More work is definitively needed to better understand what soluble ions are truly available to the rock community and

their effect on metabolism. Here, we found low amounts of nitrogen, phosphate and other trace elements but they might not be a limiting factor because very low growth rates have been reported for endolithic communities (Friedmann and Kibler 1980; Ziolkowski *et al*., 2013; Finstad *et al*., 2016). Moreover, because of high atmospheric deposition of nitrate in parts of the Atacama Desert (Friedmann and Kibler, 1980; Michalski *et al*., 2004), it has been suggested that nitrate could be a source of nitrogen for the communities. This was supported by the absence of nitrogen fixation genes in metagenomes from several endolithic communities from the Atacama Desert (Crits-Christoph *et al*., 2016a,b; Finstad *et al*., 2017). While we were not able to measure soluble iron for these substrates (because of limited amount of substrate), iron limitation would be consistent with the enrichment of genes for iron acquisition and siderophores previously described for ignimbrite and calcite substrates collected in the Atacama Desert (Crits-Christoph *et al*., 2016a). Unlike previous studies reporting microbe-mineral interactions in specific endolithic habitats (de los Ríos *et al*., 2004; 2007; Jones and Bennett, 2014; Couradeau *et al*., 2017), we did not find evidence for physico-chemical interactions between microorganisms (mostly *Cyanobacteria*) and the surrounding minerals. Neither did we find preferential adhesion of microbial cells to specific minerals. We also did not find OTUs belonging to potential chemolithoautotrophs or anoxygenic photosynthesizers, whose metabolisms can modify the pH of the microenvironment, resulting in mineral alterations (Omelon *et al*., 2007; Jones and Bennett, 2014; 2017). These findings suggest that rock chemistry in these extreme environments might not be a major driving factor for the assembly of endolithic communities.

Cyanobacteria photosynthetic activity is essential for endolithic communities and, therefore, the light intensity and wavelengths reaching the colonization zone within the endolithic habitats could be a limiting factor (Nienow *et al*., 1988; Boison *et al*., 2004; Smith *et al*., 2014; Raanan *et al*., 2016). Extremely high solar fluxes were measured in the VL and MTQ locations (up to 2554 μmol photons m^{-2} s^{-1}) but rock substrates have the capacity of drastically attenuating incident light and stopping harmful UV radiation (Berner and Evenari, 1978; Oren *et al*., 1995; Matthes *et al*., 2001; Hughes and Lawley, 2003; Horath *et al*., 2006; Amaral *et al*., 2007; Hall *et al*., 2008; Cockell *et al*., 2010; Cowan *et al*., 2011; Smith *et al*., 2014; Wierzchos *et al*., 2015). The spectral data we obtained for our four rock substrates revealed that light transmission was inversely correlated with depth of colonization. These data support the idea that light is likely the major driver for localization of the colonization zone within the rock but does not impact community's richness and diversity. If we take granite for example, its community had the lowest alpha diversity metrics of all substrates but it was more translucent than gypsum or ignimbrite, which both harboured more diverse communities. In the other hand, the most translucent rock was calcite, the substrate with the most diverse community. The transmission data we obtained for most rock substrates were within an order of magnitude to what was reported for endolithic sandstone from the Dry Valleys of Antarctica (McKay, 2012) The transmissions that we measured at 665 nm wavelength and 2 mm depth for samples of calcite, granite and gypsum were close to the 0.1% of incident light reported as the lower limit for hypolithic growth under quartz rocks from the Namib Desert (Warren-Rhodes *et al*., 2013). Samples of ignimbrite typically had less than 0.01% transmission, likewise at 665 nm wavelength and 2 mm depth. Nevertheless, our results clearly showed that differences in light properties of the rock were linked to the location and size of the colonization zone within the substrate but were not related to the richness of the communities or *Cyanobacteria's* relative abundance.

We also observed differential light transmission across wavelengths for all rocks, with higher transmission in the infrared, which is in agreement with red wavelengths penetrating deeper than blue wavelengths (McKay, 2014). Spectral tuning of photosystem II has been reported in *Cyanobacteria* (Croce and van Amerongen, 2014) and experimentally demonstrated with *Synechococcus* variants in microbial mats from hot springs (Becraft *et al*., 2015), suggesting a potential adaptation to low quantum flux densities for endolithic *Cyanobacteria*. An alternative strategy, suggested by Smith and colleagues (2014) in their study of hypolithic substrates from the Mojave Desert, might be chromatic adaptation. In this process, *Cyanobacteria* modulate the composition of primary pigments in their photosynthetic light harvesting antennae (phycobilisomes) to compensate for changes in light quality (Kehoe and Gutu, 2006).

Liquid water is essential for life and required for photosynthetic activity (Palmer and Friedmann, 1990; Lange *et al*., 1993). While our field recordings indicated similar inputs in atmospheric water for all sampling locations (rain events and RH), assessing the water available to microorganisms inside their endolithic habitat is a more difficult question. Our TWRC measurements reported a higher water retention capacity for the cryptoendolithic habitats (ignimbrite and gypsum) than for the chasmoendolithic habitats (granite and calcite). It is important to note, however, that TWRC measurements can be misleading because they are obtained from a bulk analysis that does not accurately reflect *in field* and *in situ* conditions. During the small and episodic rain events recorded in the Atacama Desert (McKay *et al*., 2003; Warren-Rhodes *et al*., 2006; Wierzchos *et al*., 2011; 2012b; 2013; 2015; DiRuggiero *et al*., 2013; Robinson *et al*., 2015), rock substrates rarely get entirely wet and definitively not totally

immersed in water (an essential step in the TWRC protocol). Additionally, the lack of information on rates of water loss by evaporation in the natural rock outcrops and gravitational infiltration processes, makes TWRC a poor indicator of water availability in natural endolithic habitat.

Conversely, the physical structure of the rock, i.e., the size of the cracks, fissures and pores and their connection to the surface, and the presence of minerals with high potential for water retention, are essential factors influencing the water retention capabilities of the rock substrate. When considering these parameters, we found that highly diverse communities were associated with substrates that have high potential for water retention (calcite and gypsum) whereas low potential for water retention was linked to low community diversity (granite and ignimbrite). For example, the presence of cracks and fractures and large pores in the gypsum allow water to penetrate easily in the substrate where it is further retained by sepiolite, a magnesium silicate clay with high efficiency for water absorption and retention (Caturla *et al.*, 1999). Indeed, the microarchitectural structure we observed in close proximity of the cells may act as a sponge, enhancing the moisture content within the gypsum rocks (Wierzchos *et al.*, 2015; Vítek *et al.*, 2016). In the calcite, a chasmoendolithic habitat, water penetrating cracks and fissures connected to the rock surface will infiltrate deeper within the rocks and be less susceptible to evaporation (DiRuggiero *et al.*, 2013). Additionally, because of the high thermal conductivity properties of calcite, dew can be formed on its surface (DiRuggiero *et al.*, 2013), thus enhancing the water budget for the community (Agam and Berliner, 2006; Büdel *et al.*, 2008; Kidron and Temina, 2013). In contrast, granite, also a chasmoendolithic habitat, is a highly weathered substrate devoid of crust, where water is easily transported in and out of the rock, thus limiting the time it is available to the community. In the cryptoendolithic habitat of ignimbrite, small bottle-shaped pores can trap water after short rainfall events. However, it has been shown that many pores were not interconnected or connected to the surface, limiting water infiltration within the matrix of substrate and thus making water scarcely accessible to microorganisms (Wierzchos *et al.*, 2013; Cámara *et al.*, 2014).

While the physical structure of the rock is an essential factor influencing the water retention capabilities of the rock substrate, the space – size and shape – available for colonization might also be an important factor impacting the habitat microenvironment. For example, in reduced space habitats, such as ignimbrite and granite, the small pores and narrow fissures might lead to diffusion limitation of nutrients and metabolic by-products within the community, thus impacting metabolic rates (Johnston and Vestal, 1991; Chan *et al.*, 2013; Ziolkowski *et al.*, 2013), community functioning, and ultimately the diversity of the microbial assemblages (Crits-Christoph *et al.*, 2016a). In ignimbrite, these diffusional constraints are exacerbated by additional stress to the community from competitions for spare resources and the effects of antimicrobial compounds (Crits-Christoph *et al.*, 2016a). In contrast, the large spaces found in gypsum and calcite rocks allow for better diffusion rates and interactions between large aggregates of microorganisms, promoting nutrient exchanges and a diversity of metabolisms (Wierzchos *et al.*, 2015; Crits-Christoph *et al.*, 2016a).

Concluding remarks

In this work, we demonstrated that distinct rock substrates, from the same climate regime and geographic area, harboured distinct microbial communities. We propose that the architecture of the rock (*sensu* Wierzchos *et al.*, 2015), i.e., the space available for colonization, embodied by the size of the cracks, fissures and pores and their connection to the surface is linked to water retention and is ultimately the driver of community diversity and composition in hyperarid desert endolithic communities. While light is essential to the primary producers of the community, reduce light transmission can be accommodated by spatial variation in colonization zones between substrates. However, further studies of endolithic communities at the functional level and using three-dimensional microscopic methods might reveal unexpected functional adaptations of community members to their unique habitat.

Experimental procedures

The following section is a summary of the Material and Methods used in this study. Detailed procedures are available in the Supporting Information.

Site description and sampling

Colonized rocks were collected in the Atacama Desert in December 2015 from two locations distant by 100 km: Valle de la Luna area (VL) (GPS coordinates 22°54'S; 068°15'W; 2619 m.a.s.l.) and Monturaqui area (MTQ) (GPS coordinates 23°57'S; 068°10'W; 2868 m.a.s.l) (Fig. 1). Both locations are plateaus (photos in Supporting Information S1) located in a N-S trending depression of the Cordon de Lila Range. These areas exhibit a pronounced rain shadow effect by the western slope of the central Andes from 15° to 23°S (DiRuggiero *et al.*, 2013; Wierzchos *et al.*, 2015). Calcite rocks were harvested in VL (Supporting Information S1-B1 and B2). Gypsum (also considered as gypcrete formation) and ignimbrite rocks were harvested in MTQ and were found side by side in the field (Supporting Information S1-C1 and C2). In MTQ area but 25 km to the west, just at the rim of the meteorite impact Monturaqui crater (GPS coordinates 23°55'S; 068°15'W; 3011 m.a.s.l.; Sanchez and Cassidy, 1966), very scarce colonized fragments of granite rocks were found sparsely distributed in the field. For each sampling location, rocks were randomly collected within a 50 m^2 area. All samples were

packed in sterile Whirlpack® bags, and stored at room temperature in the dark before further processing.

Microclimate data

Microclimate data were recorded using an Onset HOBO® Microweather Station Data Logger (H21-USB), as previously described (Wierzchos *et al.*, 2015). Air temperature (T), air relative humidity (RH in %) and Photosynthetic Active Radiation (PAR in μmol photons m^{-2} s^{-1}) were recorded from May 21st, 2013 to December 12th, 2015 (33 months) for VL. Microclimate data for MTQ were recorded from January 2011 to February 2013 (22 months) as described previously (Wierzchos *et al.*, 2015). Rainfall data for the both sampling locations were obtained from DiRuggiero *et al.* (DiRuggiero *et al.*, 2013).

Electron microscopy analyses

Colonized rock samples were processed for scanning electron microscopy in back scattered electron mode (SEM-BSE) and/or for energy dispersive X-ray spectroscopy (EDS) microanalysis according to methods by Wierzchos *et al.* (Wierzchos and Ascaso, 1994; Wierzchos *et al.*, 2011). Prepared samples (Supporting Material and Methods) were observed using a scanning electron microscope (FEI Quantum 200) equipped with a solid-state, four diodes BSE detector and an auxiliary X-ray EDS microanalytically system (INCA Oxford).

X-ray diffraction analyses

The mineralogical composition of the granite was studied by X-ray powder diffraction (XRD) using a Bruker D8 ADVANCE diffractometer with graphite-monochromated CuK(α) radiation and a linear VANTEC detector. XRD patterns were obtained from powdered samples. Phase identification was performed using the crystallographic database Powder Diffraction File (PDF-2, 1999) from the International Centre for Diffraction Data (ICDD). A semiquantitative analysis of the phases was performed using the normalized reference intensity ratio (RIR) method (Chung, 1974) and the values for each phase given by the powder diffraction database (ICDD).

Total water retention capacity and porosity

TWRC was determined on rock samples of about 5 cm^3 by total immersion of samples in H_2O at 20°C for 24 h, corresponding to the estimated time water content was constant. Dry samples were weighted prior to the experiment. Volumes of rock were measured by their immersion into water in a graduated cylinder. After 24 h, gravitational water excess was removed, and rocks were weighted again. TWRC was expressed in (%) w/w of retained water per g of rock and porosity of connected pores in (%) v/v. Duplicates were performed for calcite and gypsum substrates.

Water soluble ions analyses

Major cations and ions were analysed by Inductively Coupled Plasma-Atomic Emission Spectrometry (EPA- ICP method 200.7) and by Ion Chromatography (EPA – IC method 300.0) respectively, by Inter-Mountain Labs (Sheridan, WY, USA), using 10 grams of fine powder from each substrate, prepared as previously described (Barrett *et al.*, 2009). Duplicate samples were processed for calcite, ignimbrite and gypsum, but not for granite because of the limited number of samples available.

Light transmission measurements

Transmission of sunlight was measured using an Ocean Optics Flame-S-XR1 spectrometer (Ocean Optics, Largo, FL) with a range of 220–1025 nm and equipped with a 25 μm slit and a 600 μm optical fibre probe. A cosine corrector with a 180° field of view was placed on the optical probe. A flat-bottom hole, of the same diameter as the optical sensor (6.35 mm), was drilled in each rock from the bottom and up to 4 or 2 mm from the surface. The optical sensor equipped with the cosine corrector was placed inside the rock, flushed to the top of the hole and measurements were taken on cloudless days with the rock set up pointed at the sun. A Fresnel lens of 200 mm by 200 mm square aperture concentrated sunlight onto a 35 mm by 35 mm area of the rock surface about 60 mm beyond the focus of the lens. Each rock-and-sensor assembly was wrapped in aluminium foil, except for the sunlit surface, to prevent light intrusion from the back side of the rock. Multiple rocks of each substrate were used and several measurements were taken for each sample: (i) sun only (no Fresnel lens), (ii) rock only (no Fresnel lens), (iii) rock + Fresnel lens and (iv) dark controls (caps on top of rock and sensor), and up to 10 spectra were taken for each measurement. The transmission t for each rock was computed as

$$t = S(\text{Rock})/S(\text{Sun})$$

where S(Rock) is a vector representing the calibrated spectrum taken with sun light incident on the 'front' face of the rock opposite the side into which we inserted the fibre probe into the hole and S(Sun) is a similarly formed calibrated spectrum taken with the rock removed, leaving the fibre probe aimed at the Sun and the day-time sky. The Data Reduction section is in Supporting Information S4.

DNA extraction procedures

At least 4 individual rocks were processed per substrate totalizing 47 samples. The width, maximum and minimum depth of the colonization zone were measured for each substrate before scraping and grounding the colonization zone for DNA extraction. For calcite, ignimbrite and granite, DNA extraction was performed using 0.25g of samples and the PowerSoil kit (MoBio Laboratories, Solana Beach, CA, USA), following the manufacturer's recommendations. For gypsum samples, we designed a custom protocol by combining sonication, enzymatic lysis and the PowerBiofilm kit (MoBio Laboratories), with minor modifications (Supporting Material and Methods). All DNA concentrations were measured with the Qubit fluorometer dsDNA HS Assay kit (Life Technologies, Carlsbad, CA). Ignimbrite rocks (n = 3) were processed using both protocols to validate the robustness of the DNA isolation procedures

and DNA duplicates were processed to validate the robustness of the analytical pipeline (Supporting Information S3).

16S rRNA gene libraries preparation and sequencing

A two-step PCR strategy was used to prepare the sequencing libraries, as previously described (Robinson *et al*., 2015). DNA was amplified using primers 338F and 806R (V3-V4 hypervariable region) barcoded for multiplexing; amplicons from 2 PCR reactions were pooled after the first step. Illumina paired-end sequencing (2×250bp) was performed using the MiSeq platform at the Johns Hopkins Genetic Resources Core Facility (GRCF), Libraries from 3 samples were used on all sequencing runs to test for batch effect (Supporting Information S3).

Computational analysis

After demultiplexing and barcode removal, sequence reads with phred score < 20 and length < 100bp were discarded using sickle (Joshi and Fass, 2011), representing only 2% of the initial reads count. The Qiime package (v1.6.0) was used to further process the sequences (Caporaso *et al*., 2010) and diversity metrics were calculated based on OTUs at the 0.03% cutoff against the SILVA database release 123 (Quast *et al*., 2013). The resulting OTUs table was filtered of the rare OTUs (total abundance across all samples $\leq 0.2\%$), representing 29% of the initial count (1183 OTUs). Spearman correlations were performed using cor() in R.

The 30% most abundant OTUs for *Cyanobacteria* and *Actinobacteria* were analysed with R using the pheatmap (Kolde, 2015) and DESeq2 packages (Love *et al*., 2014). Main OTUs were aligned in NCBI GenBank using Clustal W 1.4 software (Thompson *et al*., 1994. Phylogenetic trees were constructed in MEGA 6.0 using the Maximum Likelihood method (Tamura *et al*., 2011) and the Kimura 2-parameter model (Kimura, 1980). Trees were finally visualized and annotated using the iTOL tool (Letunic and Bork, 2016).

Data submission

The data sets supporting the results of this article are available National Centre for Biotechnology Information under BioSample numbers SAMN07500207-253 and SAMN07519406-418 and BioProject ID PRJNA398025.

Acknowledgements

This work was funded by grants NNX15AP18G and NNX15AK57G from NASA, grant DEB1556574 from the NSF to JDR and grant CGL2013-42509P from the Spanish Ministry of Economy, Industry and Competitiveness to JW, CA, OA, JDR and MCC. The MNCN-CSIC, Madrid, Spain is acknowledged for microscopy services. We thank Kate Sacchi from Ocean Optics for her support.

Author Contributions

VM and JDR designed and performed the research and wrote the manuscript. JDR and JW conceived the original project. JW and CA performed the microscopy; OA performed the chemical and mineralogy analyses; PRM and JDR performed the light transmission spectroscopy and PRM performed the analysis of the data and wrote the associated text; MCC and MD contributed to the molecular data and analysis; JDR, VM, JW, CA, OA and MCC participated in sampling and microclimate data acquisition. All authors contributed to editing and revising the manuscript and approved this version for submission.

References

Agam, N., and Berliner, P.R. (2006) Dew formation and water vapor adsorption in semi-arid environments—a review. *J Arid Environ* **65:** 572–590.

Amaral, G., Martinez-Frias, J., and Vazquez, L. (2007) UV shielding properties of jarosite vs gypsum: astrobiological implications for mars. *World Appl Sci J* **2:** 112–116.

Archer, S.D.J., de los Ríos, A., Lee, K.C., Niederberger, T.S., Cary, S.C., and Coyne, K.J. (2017) Endolithic microbial diversity in sandstone and granite from the McMurdo Dry Valleys, Antarctica. *Polar Biol* **40:** 997–1006.

Armstrong, A., Valverde, A., Ramond, J.-B., Makhalanyane, T.P., Jansson, J.K., Hopkins, D.W., *et al*. (2016) Temporal dynamics of hot desert microbial communities reveal structural and functional responses to water input. *Sci Rep* **6:** 34434.

Ascaso, C., and Wierzchos, J. (2002) New approaches to the study of Antarctic lithobiontic microorganisms and their inorganic traces, and their application in the detection of life in Martian rocks. *Int Microbiol* **5:** 215–222.

Azúa-Bustos, A., González-Silva, C., Mancilla, R.A., Salas, L., Gómez-Silva, B., McKay, C.P., and Vicuña, R. (2011) Hypolithic cyanobacteria supported mainly by fog in the coastal range of the Atacama Desert. *Microb Ecol* **61:** 568–581.

Barrett, J., Ball, B., and Simmons, B. (2009) Standard Procedures for Soil Research in the McMurdo Dry Valleys LTER. pp. 1–32.

Becraft, E.D., Wood, J.M., Rusch, D.B., Kühl, M., Jensen, S.I., Bryant, D.A., *et al*. (2015) The molecular dimension of microbial species: 1. Ecological distinctions among, and homogeneity within, putative ecotypes of Synechococcus inhabiting the cyanobacterial mat of Mushroom Spring, Yellowstone National Park. *Front Microbiol* **6:** 590.

Bell, R.A., Athey, P.V., and Sommerfeld, M.R. (1986) Cryptoendolithic algal communities of the Colorado Plateau. *J Phycol* **22:** 429–435.

Berner, T., and Evenari, M. (1978) The influence of temperature and light penetration on the abundance of the hypolithic algae in the Negev Desert of Israel. *Oecologia* **33:** 255–260.

Billi, D., Friedmann, E.I., Hofer, K.G., Caiola, M.G., and Ocampo-Friedmann, R. (2000) Ionizing-radiation resistance in the desiccation-tolerant cyanobacterium Chroococcidiopsis. *Appl Environ Microbiol* **66:** 1489–1492.

Boison, G., Mergel, A., Jolkver, H., and Bothe, H. (2004) Bacterial life and dinitrogen fixation at gysum rock. *Appl Environ Microbiol* **70:** 7070–7077.

Büdel, B., Bendix, J., Bicker, F.R., and Allan Green, T.G. (2008) Dewfall as a water source frequently activates the endolithic cyanobacterial communities in the granites of Taylor Valley, Antarctica. *J Phycol* **44:** 1415–1424.

Bull, A.T. (2011) Actinobacteria of the extremobiosphere. In *Extremophiles Handbook*. Koki, H. (ed). Tokyo, Japan Springer, pp. 1203–1240.

Cámara, B., Suzuki, S., Nealson, K.H., Wierzchos, J., Ascaso, C., Artieda, O., and de los Ríos, A. (2014) Ignimbrite textural properties as determinants of endolithic colonization patterns from hyper-arid Atacama Desert. *Int Microbiol* **17:** 235–247.

Canfora, L., Vendramin, E., Vittori Antisari, L., Lo Papa, G., Dazzi, C., Benedetti, A., *et al*. (2016) Compartmentalization of gypsum and halite associated with cyanobacteria in saline soil crusts. *FEMS Microbiol Ecol* **92:** fiw080.

Caporaso, J.G., Kuczynski, J., Stombaugh, J., Bittinger, K., Bushman, F.D., Costello, E.K., *et al*. (2010) QIIME allows analysis of high-throughput community sequencing data. *Nat Methods* **7:** 335–336.

Cary, S.C., McDonald, I.R., Barrett, J.E., and Cowan, D.A. (2010) On the rocks: the microbiology of Antarctic Dry Valley soils. *Nat Rev Microbiol* **8:** 129–138.

Caturla, F., Molina-Sabio, M., and Rodriguez-Reinoso, F. (1999) Adsorption–desorption of water vapor by natural and heat-treated sepiolite in ambient air. *Appl Clay Sci* **15:** 367–380.

Chan, Y., Van Nostrand, J.D., Zhou, J., Pointing, S.B., and Farrell, R.L. (2013) Functional ecology of an Antarctic Dry Valley. *Proc Natl Acad Sci U. S. A* **110:** 8990–8995.

Chung, F.H. (1974) Quantitative interpretation of X-ray diffraction patterns of mixtures. II. Adiabatic principle of X-ray diffraction analysis of mixtures. *J Appl Crystallogr* **7:** 526–531.

Cockell, C.S., McKay, C.P., and Omelon, C. (2002) Polar endoliths - an anti-correlation of climatic extremes and microbial biodiversity. *Int J Astrobiol* **1:** 305–310.

Cockell, C.S., Osinski, G.R., Banerjee, N.R., Howard, K.T., Gilmour, I., and Watson, J.S. (2010) The microbe-mineral environment and gypsum neogenesis in a weathered polar evaporite. *Geobiology* **8:** 293–308.

Cordero, R.R., Seckmeyer, G., Damiani, A., Riechelmann, S., Rayas, J., Labbe, F., and Laroze, D. (2014) The world's highest levels of surface UV. *Photochem Photobiol Sci* **13:** 70–81.

Couradeau, E., Roush, D., Guida, B.S., and Garcia-Pichel, F. (2017) Diversity and mineral substrate preference in endolithic microbial communities from marine intertidal outcrops (Isla de Mona, Puerto Rico). *Biogeosciences* **14:** 311–324.

Cowan, D.A., Pointing, S.B., Stevens, M.I., Craig Cary, S., Stomeo, F., and Tuffin, I.M. (2011) Distribution and abiotic influences on hypolithic microbial communities in an Antarctic Dry Valley. *Polar Biol* **34:** 307–311.

Crits-Christoph, A., Robinson, C.K., Ma, B., Ravel, J., Wierzchos, J., Ascaso, C., *et al*. (2016a) Phylogenetic and functional substrate specificity for endolithic microbial communities in hyper-arid environments. *Front Microbiol* **7:** 301.

Crits-Christoph, A., Gelsinger, D.R., Ma, B., Wierzchos, J., Ravel, J., Davila, A., *et al*. (2016b) Functional interactions of archaea, bacteria and viruses in a hypersaline endolithic community. *Environ Microbiol* **18:** 2064–2077.

Croce, R., and van Amerongen, H. (2014) Natural strategies for photosynthetic light harvesting. *Nat Chem Biol* **10:** 492–501.

Davila, A.F., Gómez-Silva, B., de los Rios, A., Ascaso, C., Olivares, H., McKay, C.P., and Wierzchos, J. (2008) Facilitation of endolithic microbial survival in the hyperarid core of the Atacama Desert by mineral deliquescence. *J Geophys Res* **113:** G01028.

DiRuggiero, J., Wierzchos, J., Robinson, C.K., Souterre, T., Ravel, J., Artieda, O., *et al*. (2013) Microbial colonisation of chasmoendolithic habitats in the hyper-arid zone of the Atacama Desert. *Biogeosciences* **10:** 2439–2450.

Dong, H., Rech, J.A., Jiang, H., Sun, H., and Buck, B.J. (2007) Endolithic cyanobacteria in soil gypsum: occurrences in Atacama (Chile), Mojave (United States), and Al-Jafr Basin (Jordan) deserts. *J Geophys Res* **112:** G02030.

Finstad, K., Pfeiffer, M., McNicol, G., Barnes, J., Demergasso, C., Chong, G., and Amundson, R. (2016) Rates and geochemical processes of soil and salt crust formation in Salars of the Atacama Desert, Chile. *Geoderma* **284:** 57–72.

Finstad, K.M., Probst, A.J., Thomas, B.C., Andersen, G.L., Demergasso, C., Echeverría, A., *et al*. (2017) Microbial community structure and the persistence of cyanobacterial populations in salt crusts of the hyperarid Atacama desert from genome-resolved metagenomics. *Front Microbiol* **8:** 1–10.

Friedmann, E.I. (1980) Endolithic microbial life in hot and cold deserts. *Orig Life* **10:** 223–235.

Friedmann, E.I. (1982) Endolithic microorganisms in the antarctic cold desert. *Science* **215:** 1045–1053.

Friedmann, E.I., and Kibler, A.P. (1980) Nitrogen economy of endolithic microbial communities in hot and cold deserts. *Microb Ecol* **6:** 95–108.

Friedmann, E.I., and Ocampo-Friedmann, R. (1995) A primitive cyanobacterium as pioneer microorganism for terraforming Mars. *Adv Space Res* **15:** 243–246.

Friedmann, E.I., Hua, M., and Ocampo-Friedmann, R. (1988) Cryptoendolithic lichen and cyanobacterial communities of the Ross Desert, Antarctica. *Polarforschung* **58:** 251–259.

Golubic, S., Friedmann, E.I., and Schneider, J. (1981) The lithobiontic ecological niche, with special reference to microorganisms. *J Sediment Res* **51:** 475–478.

Hall, K., Guglielmin, M., and Strini, A. (2008) Weathering of granite in Antarctica: I. Light penetration into rock and implications for rock weathering and endolithic communities. *Earth Surf Process Landforms* **33:** 295–307.

Horath, T., Neu, T.R., and Bachofen, R. (2006) An endolithic microbial community in dolomite rock in central Switzerland: characterization by reflection spectroscopy, pigment analyses, scanning electron microscopy, and laser scanning microscopy. *Microb Ecol* **51:** 353–364.

Houston, J., and Hartley, A. (2003) The central Andean west-slope rainshadow and its potential contribution to the origin of hyper-aridity in the Atacama Desert. *Int J Climatol* **23:** 1453–1464.

Hughes, K.A., and Lawley, B. (2003) A novel Antarctic microbial endolithic community within gypsum crusts. *Environ Microbiol* **5:** 555–565.

Johnston, C.G., and Vestal, J.R. (1991) Photosynthetic carbon incorporation and turnover in antarctic cryptoendolithic microbial communities: are they the slowest-growing communities on Earth?. *Appl Environ Microbiol* **57:** 2308–2311.

Jones, A.A., and Bennett, P.C. (2014) Mineral microniches control the diversity of subsurface microbial populations. *Geomicrobiol J* **31:** 246–261.

Jones, A.A., and Bennett, P.C. (2017) Mineral ecology: surface specific colonization and geochemical drivers of biofilm

accumulation, composition, and phylogeny. *Front Microbiol* **8:** 491.

Joshi, N.A., and Fass, J.N. (2011) *Sickle: a sliding-window, adaptive, quality-based trimming tool for FastQ files (version 1.33) [Software]*. [WWW document]. URL https://github.com/najoshi/sickle

Kehoe, D.M., and Gutu, A. (2006) Responding to color: the regulation of complementary chromatic adaptation. *Annu Rev Plant Biol* **57:** 127–150.

Kidron, G.J., and Temina, M. (2013) The effect of dew and fog on lithic lichens along an altitudinal gradient in the Negev Desert. *Geomicrobiol J* **30:** 281–290.

Kidron, G.J., and Temina, M. (2017) Non-rainfall water input determines lichen and cyanobacteria zonation on limestone bedrock in the Negev Highlands. *Flora* **229:** 71–79.

Kimura, M. (1980) A simple method for estimating evolutionary rates of base substitutions through comparative studies of nucleotide sequences. *J Mol Evol* **16:** 111–120.

Kolde, R. (2015) *pheatmap: pretty Heatmaps. R package (version 1.0.8.) [software]*. [WWW document]. URL http://CRAN.R-projetcs.org/package=pheatmap.

Krisko, A., and Radman, M. (2013) Biology of extreme radiation resistance: the way of Deinococcus radiodurans. *Cold Spring Harb Perspect Biol* **5:** a012765.

Lacap-Bugler, D.C., Lee, K.K., Archer, S., Gillman, L.N., Lau, M.C.Y., Leuzinger, S., *et al*. (2017) Global diversity of desert hypolithic cyanobacteria. *Front Microbiol* **8:** 1–13.

Lange, O.L., Budel, B., Meyer, A., and Kilian, E. (1993) Further evidence that activation of photosyntesis by dry cyanobacterial lichens requires liquid water. *Lichenologist* **25:** 175–189.

Lebre, P.H., De Maayer, P., and Cowan, D.A. (2017) Xerotolerant bacteria: surviving through a dry spell. *Nat Rev Microbiol* **15:** 285–296.

Lee, K.C., Archer, S.D.J., Boyle, R.H., Lacap-Bugler, D.C., Belnap, J., and Pointing, S.B. (2016) Niche filtering of bacteria in soil and rock habitats of the Colorado Plateau Desert, Utah, USA. *Front Microbiol* **7:** 1489.

Letunic, I., and Bork, P. (2016) Interactive tree of life (iTOL) v3: an online tool for the display and annotation of phylogenetic and other trees. *Nucleic Acids Res* **44:** W242–W245.

Li, S., Shi, Y., Zhang, Q., Liao, X., Zhu, L., and Lou, K. (2013) Phylogenetic diversity of endolithic bacteria in Bole granite rock in Xinjiang. *Acta Ecol Sin* **33:** 178–184.

Love, M.I., Huber, W., and Anders, S. (2014) Moderated estimation of fold change and dispersion for RNA-seq data with DESeq2. *Genome Biol* **15:** 550.

Makhalanyane, T.P., Valverde, A., Lacap, D.C., Pointing, S.B., Tuffin, M.I., and Cowan, D.A. (2013) Evidence of species recruitment and development of hot desert hypolithic communities. *Environ Microbiol Rep* **5:** 219–224.

Matthes, U., Turner, S.J., and Larson, D.W. (2001) Light attenuation by limestone rock and its constraint on the depth distribution of endolithic algae and cyanobacteria. *Int J Plant Sci* **162:** 263–270.

McKay, C.P. (2012) Full solar spectrum measurements of absorption of light in a sample of the Beacon Sandstone containing the Antarctic cryptoendolithic microbial community. *Antarctic Sci* **24:** 243–248.

McKay, C.P. (2014) Requirements and limits for life in the context of exoplanets. *Proc Natl Acad Sci USA* **111:** 12628–12633.

McKay, C.P., and Friedmann, E.I. (1985) The cryptoendolithic microbial environment in the Antarctic cold desert: temperature variations in nature. *Polar Biol* **4:** 19–25.

McKay, C.P., Friedmann, E.I., Gómez-Silva, B., Cáceres-Villanueva, L., Andersen, D.T., and Landheim, R. (2003) Temperature and moisture conditions for life in the extreme arid region of the Atacama Desert: four years of observations including the El Niño of 1997–1998. *Astrobiology* **3:** 393–406.

Michalski, G., Böhlke, J.K., and Thiemens, M. (2004) Long term atmospheric deposition as the source of nitrate and other salts in the Atacama Desert, Chile: new evidence from mass-independent oxygen isotopic compositions. *Geochim Cosmochim Acta* **68:** 4023–4038.

Mohammadipanah, F., and Wink, J. (2016) Actinobacteria from arid and desert habitats: diversity and biological activity. *Front Microbiol* **6:** 1541.

Nienow, J.A., McKay, C.P., and Friedmann, E.I. (1988) The cryptoendolithic microbial environment in the Ross Desert of Antarctica: light in the photosynthetically active region. *Microb Ecol* **16:** 271–289.

Omelon, C.R. (2008) Endolithic microbial communities in polar desert habitats. *Geomicrobiol J* **25:** 404–414.

Omelon, C.R., Pollard, W.H., and Ferris, F.G. (2006) Environmental controls on microbial colonization of high Arctic cryptoendolithic habitats. *Polar Biol* **30:** 19–29.

Omelon, C.R., Pollard, W.H., and Ferris, F.G. (2007) Inorganic species distribution and microbial diversity within high Arctic cryptoendolithic habitats. *Microb Ecol* **54:** 740–752.

Oren, A., Kühl, M., and Karsten, U. (1995) An endoevaporitic microbial mat within a gypsum crust: zonation of phototrophs, photopigments, and light penetration. *Mar Ecol Prog Ser* **128:** 151–159.

Palmer, R.J., and Friedmann, E.I. (1990) Water relations, thallus structure and photosynthesis in Negev Desert lichens. *New Phytol* **116:** 597–603.

Pointing, S.B., Warren-Rhodes, K.A., Lacap, D.C., Rhodes, K.L., and McKay, C.P. (2007) Hypolithic community shifts occur as a result of liquid water availability along environmental gradients in China's hot and cold hyperarid deserts. *Environ Microbiol* **9:** 414–424.

Pointing, S.B., Chan, Y., Lacap, D.C., Lau, M.C.Y., Jurgens, J.A., and Farrell, R.L. (2009) Highly specialized microbial diversity in hyper-arid polar desert. *Proc Natl Acad Sci U S A* **106:** 19964–19969.

Potts, M. (1999) Mechanisms of desiccation tolerance in cyanobacteria. *Eur J Phycol* **34:** 319–328.

Quast, C., Pruesse, E., Yilmaz, P., Gerken, J., Schweer, T., Yarza, P., *et al*. (2013) The SILVA ribosomal RNA gene database project: improved data processing and web-based tools. *Nucleic Acids Res* **41:** D590–D596.

Raanan, H., Felde, V.J.M.N.L., Peth, S., Drahorad, S., Ionescu, D., Eshkol, G., *et al*. (2016) Three-dimensional structure and cyanobacterial activity within a desert biological soil crust. *Environ Microbiol* **18:** 372–383.

de los Ríos, A., Wierzchos, J., Sancho, L.G., and Ascaso, C. (2004) Exploring the physiological state of continental Antarctic endolithic microorganisms by microscopy. *FEMS Microbiol Ecol* **50:** 143–152.

de los Ríos, A., Wierzchos, J., Sancho, L.G., Green, T.G.A., and Ascaso, C. (2005) Ecology of endolithic

lichens colonizing granite in continental Antarctica. *Lichenologist* **37:** 383.
de los Ríos, A., Grube, M., Sancho, L.G., and Ascaso, C. (2007) Ultrastructural and genetic characteristics of endolithic cyanobacterial biofilms colonizing Antarctic granite rocks. *FEMS Microbiol Ecol* **59:** 386–395.
de los Ríos, A., Valea, S., Ascaso, C., Davila, A., Kastovsky, J., McKay, C.P., *et al*. (2010) Comparative analysis of the microbial communities inhabiting halite evaporites of the Atacama Desert. *Int Microbiol* **13:** 79–89.
Robinson, C.K., Wierzchos, J., Black, C., Crits-Christoph, A., Ma, B., Ravel, J., *et al*. (2015) Microbial diversity and the presence of algae in halite endolithic communities are correlated to atmospheric moisture in the hyper-arid zone of the Atacama Desert. *Environ Microbiol* **17:** 299–315.
Sanchez, J., and Cassidy, W. (1966) A previously undescribed Meteorite Crater in Chile. *J Geophys Res* **71:** 4891–4895.
Sawyer, D.J., McGehee, M.D., Canepa, J., and Moore, C.B. (2000) Water soluble ions in the Nakhla martian meteorite. *Meteorit Planet Sci* **35:** 743–747.
Smith, H.D., Baqué, M., Duncan, A.G., Lloyd, C.R., McKay, C.P., and Billi, D. (2014) Comparative analysis of cyanobacteria inhabiting rocks with different light transmittance in the Mojave Desert: a Mars terrestrial analogue. *Int J Astrobiol* **13:** 271–277.
Stivaletta, N., López-García, P., Boihem, L., Millie, D.F., and Barbieri, R. (2010) Biomarkers of endolithic communities within gypsum crusts (Southern Tunisia). *Geomicrobiol J* **27:** 101–110.
Stomeo, F., Valverde, A., Pointing, S.B., McKay, C.P., Warren-Rhodes, K.A., Tuffin, M.I., *et al*. (2013) Hypolithic and soil microbial community assembly along an aridity gradient in the Namib Desert. *Extremophiles* **17:** 329–337.
Tait, A.W., Gagen, E.J., Wilson, S.A., Tomkins, A.G., and Southam, G. (2017) Microbial populations of stony meteorites: substrate controls on first colonizers. *Front Microbiol* **8:** 1–14.
Tamura, K., Peterson, D., Peterson, N., Stecher, G., Nei, M., and Kumar, S. (2011) MEGA5: molecular evolutionary genetics analysis using maximum likelihood, evolutionary distance, and maximum parsimony methods. *Mol Biol Evol* **28:** 2731–2739.
Tang, Y., Lian, B., Dong, H., Liu, D., and Hou, W. (2012) Endolithic bacterial communities in Dolomite and Limestone rocks from the Nanjiang Canyon in Guizhou Karst Area (China). *Geomicrobiol J* **29:** 213–225.
Tang, Y., Cheng, J., and Lian, B. (2016) Characterization of endolithic culturable microbial communities in carbonate rocks from a typical Karst Canyon in Guizhou (China). *Polish J Microbiol* **65:** 413–423.
Thompson, J.D., Higgins, D.G., and Gibson, T.J. (1994) CLUSTAL W: improving the sensitivity of progressive multiple sequence alignment through sequence weighting, position-specific gap penalties and weight matrix choice. *Nucleic Acids Res* **22:** 4673–4680.
Toner, J.D., Sletten, R.S., and Prentice, M.L. (2013) Soluble salt accumulations in Taylor Valley, Antarctica: Implications for paleolakes and Ross Sea Ice Sheet dynamics. *J Geophys Res* **118:** 198–215.
de la Torre, J.R., Goebel, B.M., Friedmann, E.I., and Pace, N.R. (2003) Microbial diversity of cryptoendolithic communities from the McMurdo Dry Valleys, Antarctica. *Appl Environ Microbiol* **69:** 3858–3867.
Valverde, A., Makhalanyane, T.P., Seely, M., and Cowan, D.A. (2015) Cyanobacteria drive community composition and functionality in rock-soil interface communities. *Mol Ecol* **24:** 812–821.
Vítek, P., Ascaso, C., Artieda, O., and Wierzchos, J. (2016) Raman imaging in geomicrobiology: endolithic phototrophic microorganisms in gypsum from the extreme sun irradiation area in the Atacama Desert. *Anal Bioanal Chem* **408:** 4083–4092.
Walker, J.J., and Pace, N.R. (2007) Endolithic microbial ecosystems. *Annu Rev Microbiol* **61:** 331–347.
Walker, J.J., Spear, J.R., and Pace, N.R. (2005) Geobiology of a microbial endolithic community in the Yellowstone geothermal environment. *Nature* **434:** 1011–1014.
Warren-Rhodes, K. A., Rhodes, K.L., Pointing, S.B., Ewing, S. A., Lacap, D.C., and Gómez-Silva, B. (2006) Hypolithic cyanobacteria, dry limit of photosynthesis, and microbial ecology in the hyperarid Atacama Desert. *Microb Ecol* **52:** 389–398.
Warren-Rhodes, K.A., McKay, C.P., Boyle, L.N., Wing, M.R., Kiekebusch, E.M., Cowan, D.A., *et al*. (2013) Physical ecology of hypolithic communities in the central Namib Desert: The role of fog, rain, rock habitat, and light. *J Geophys Res* **118:** 1451–1460.
Wierzchos, J., and Ascaso, C. (1994) Application of backscattered electron imaging to the study of the lichen-rock interface. *J Microsc* **175:** 54–59.
Wierzchos, J., and Ascaso, C. (2001) Life, decay and fossilisation of endolithic microorganisms from the Ross Desert, Antarctica. *Polar Biol* **24:** 863–868.
Wierzchos, J., Ascaso, C., and McKay, C.P. (2006) Endolithic cyanobacteria in halite rocks from the hyperarid core of the Atacama Desert. *Astrobiology* **6:** 415–422.
Wierzchos, J., Cámara, B., de los Ríos, A., Davila, A.F., Sánchez Almazo, I.M., Artieda, O., *et al*. (2011) Microbial colonization of Ca-sulfate crusts in the hyperarid core of the Atacama Desert: implications for the search for life on Mars. *Geobiology* **9:** 44–60.
Wierzchos, J., de los Ríos, A., and Ascaso, C. (2012a) Microorganisms in desert rocks: the edge of life on earth. *Int Microbiol* **15:** 173–183.
Wierzchos, J., Davila, A.F., Sánchez-Almazo, I.M., Hajnos, M., Swieboda, R., and Ascaso, C. (2012b) Novel water source for endolithic life in the hyperarid core of the Atacama Desert. *Biogeosciences* **9:** 2275–2286.
Wierzchos, J., Davila, A.F., Artieda, O., Cámara-Gallego, B., de los Ríos, A., Nealson, K.H., *et al*. (2013) Ignimbrite as a substrate for endolithic life in the hyper-arid Atacama Desert: implications for the search for life on Mars. *Icarus* **224:** 334–346.
Wierzchos, J., DiRuggiero, J., Vítek, P., Artieda, O., Souza-Egipsy, V., Škaloud, P., *et al*. (2015) Adaptation strategies of endolithic chlorophototrophs to survive the hyperarid and extreme solar radiation environment of the Atacama Desert. *Front Microbiol* **6:** 934.
Wierzchos, J., Casero, M.C., Artieda, O., and Ascaso, C. (2018) Endolithic microbial habitats as refuges for life in

polyextreme environment of the Atacama Desert. *Curr Opin Microbiol* **43:** 124–131.

Ziolkowski, L.A., Wierzchos, J., Davila, A.F., and Slater, G.F. (2013) Radiocarbon evidence of active endolithic microbial communities in the hyperarid core of the Atacama Desert. *Astrobiology* **13:** 607–616.

Supporting information

Additional Supporting Information may be found in the online version of this article at the publisher's web-site:

Materials and Methods

S1. Landscapes in Valle de la Luna and Monturaqui.

S2. Validation of our experimental pipeline.

S3. Water soluble ions analysis, TWRC and Porosity analysis

S4. Substrate light transmission spectra

S5. Alpha-diversity metrics and rarefaction curves with OTU clustering at 97%.

S6. Box plots of the relative abundance for *Chloroflexi* and *Proteobacteria*

S7. Occurrence and relative abundance of phyla detected in each substrate type.

S8. PCoA plots for beta-diversity pairwise distance matrices for all samples.

S9. Heatmap (A) and Volcano Plot (B) of the 30% most abundant *Actinobacteria* OTUs.

S10. Maximum Likelihood trees of the 30% most abundant *Cyanobacteria* (A) and *Actinobacteria* (B) across samples.